

Lodz University of Technology

SCIENTIFIC BULLETIN

PHYSICS

Vol. 40

LODZ 2019

LODZ UNIVERSITY OF TECHNOLOGY

SCIENTIFIC BULLETIN

No. 1227

PHYSICS

Vol. 40

LODZ 2019

ZESZYTY NAUKOWE POLITECHNIKI ŁÓDZKIEJ
SCIENTIFIC BULLETIN OF THE LODZ UNIVERSITY OF TECHNOLOGY
BULLETIN SCIENTIFIQUE
DE L'UNIVERSITÉ POLYTECHNIQUE DE LODZ
НАУЧНЫЕ ЗАПИСКИ
ЛОДЗИНСКОГО ПОЛИТЕХНИЧЕСКОГО УНИВЕРСИТЕТА
WISSENSCHAFTLICHE HEFTE
DER TECHNISCHEN UNIVERSITÄT IN LODZ

Editor of series: **Mariola Buczkowska, Ph.D., D.Sc., Eng.**

© Copyright by Politechnika Łódzka 2019

Adres Redakcji – Адрес Редакции – Editor's Office
Adresse de Redaction – Schriftleitungsadresse:

WYDAWNICTWO POLITECHNIKI ŁÓDZKIEJ

90-924 Łódź, ul. Wólczańska 223

tel. 42-631-20-87, 42-631-29-52

e-mail: zamowienia@info.p.lodz.pl

www.wydawnictwo.p.lodz.pl

ISSN 1505-1013

e-ISSN 2449-982X

doi:10.34658/physics.2019.40

<https://doi.org/10.34658/physics.2019.40>

<http://cybra.lodz.pl/publication/3923>

<http://czasopisma.p.lodz.pl/PHYSICS/issue/archive>

Mariola Buczkowska – Influence of chirality on two-dimensional deformations of twisted flexoelectric nematic layers	5-12
Sylwester Kania, Janusz Kuliński, Dominik Sikorski – Electrical and thermal properties of anthraquinone layers.....	13-25
Sylwester Kania, Barbara Kościelniak-Mucha, Janusz Kuliński, Piotr Słoma, Krzysztof Wojciechowski – Polarization of organic aromatic molecule in anionic and cationic state.....	27-35
Sylwester Kania, Barbara Kościelniak-Mucha, Janusz Kuliński, Piotr Słoma, Krzysztof Wojciechowski – Charge carrier mobility in non-equilibrated transport in molecular materials	37-46

MARIOLA BUCZKOWSKA

Institute of Physics, Lodz University of Technology, ul. Wólczańska 219,
90-924 Łódź, Poland, e-mail: mariola.buczowska@p.lodz.pl

INFLUENCE OF CHIRALITY ON TWO-DIMENSIONAL DEFORMATIONS IN TWISTED FLEXOELECTRIC NEMATIC LAYERS

Two-dimensional deformations induced by electric field in twisted nematic cells filled with liquid crystal possessing flexoelectric properties were simulated numerically. The influence of chiral dopants on the occurrence and structure of the spatially periodic patterns was investigated. It was found that the chirality influences mainly the direction of the periodic patterns whereas the threshold voltage for deformation and the width of the stripes are weakly affected.

Keywords: twisted nematic, flexoelectricity, chirality, periodic patterns.

1. INTRODUCTION

Thin layers of nematic liquid crystals confined between plane-parallel electrodes are fundamental for construction of displays and of other liquid crystal devices [1]. The twisted nematic cells in which the undistorted director remains parallel to the boundary plates but is twisted by $\Phi = 90^\circ$ along the normal to the layer are the most common. The structure twisted by 90° is achieved due to suitable surface anchoring which determines the easy axes oriented in mutually crossed directions. The twisted structure arises if the layer is filled with pure nematic material or if it is doped with some chiral substance which imposes some intrinsic pitch p . The chirality, defined as $q = 2\pi/p$, should range between 0 and $\pi/(2d)$. In the latter case, the intrinsic pitch is compatible with the twist angle Φ .

General principle of operation of the twisted nematic cells consists in electric field induced deformations of director orientation. Two kinds of distortions are possible: one-dimensional, *i.e.* homogeneous over the whole area of the electrodes and two-dimensional in which the director orientation depends

not only on the coordinate normal to the layer but it also varies along some direction parallel to the layer [2, 3]. The two-dimensional deformations are spatially periodic. They are visible under microscope in the form of parallel stripes. They also destroy homogeneous appearance of the area of an excited pixel of a display, therefore are undesirable.

The influence of electric field on director distribution is due to dielectric anisotropy and to flexoelectricity of the nematic material [4, 5]. The occurrence of one- and two-dimensional deformations induced in pure nematic substance ($q = 0$) was studied in the earlier paper [3, 6]. It was found that if the nematic possesses sufficiently strong flexoelectric properties, then the spatially periodic deformations appear since they have smaller free energy than the homogeneous deformations. This is interesting because flexoelectricity can become essential feature of a nematic mixture if it contains mesogenic substances composed of bent-core molecules which exhibit giant flexoelectric properties [7, 8]. The stripes are characterized by their width λ and by the angle ψ which they make with the direction of the mid-plane director orientation in the undistorted structure. Two types of stripes were distinguished which differ in structure and direction [3].

The aim of the present paper is to study the role of chirality for arising of the stripes. Various values of the chirality were taken into account.

2. ASSUMPTIONS AND METHOD

The nematic structure of thickness $d = 6 \mu\text{m}$ confined between two plane electrodes parallel to the xy plane of Cartesian coordinate system positioned at $z = \pm d/2$ and twisted by $\Phi = 90^\circ$ was considered. We assumed that all the physical quantities and variables describing the two dimensional structures depended on two coordinates, y and z , and were constant along the x axis. The director orientation $\mathbf{n}(y, z)$ was determined by means of the polar angle $\theta(y, z)$ measured between \mathbf{n} and the xy plane and by the azimuthal angle $\phi(y, z)$ made between the x axis and the projection of \mathbf{n} on the xy plane. Voltage U was applied between the electrodes. The lower electrode was earthed, *i.e.* potential $V(-d/2) = 0$. Boundary conditions were determined by the polar and azimuthal angles $\theta_{s1} = \theta_{s2} = 0$, $\phi_{s1} = -45^\circ$ and $\phi_{s2} = 45^\circ$ which determined orientation of the easy axes \mathbf{e}_1 and \mathbf{e}_2 on the lower and upper electrode, respectively. The anisotropic surface anchoring, expressed by the formula proposed in [9], was assumed. The anchoring energy was determined by polar and azimuthal anchoring strengths, $W_{\theta 1} = W_{\theta 2} = 10^{-4} \text{ J/m}^2$, $W_{\phi 1} = W_{\phi 2} = 10^{-5} \text{ J/m}^2$. The elastic

constants of the nematic were $k_{11} = 8$ pN, $k_{22} = 3$ pN, $k_{33} = 10$ pN. Small positive dielectric anisotropy $\Delta\epsilon = 2$ was assumed. Flexoelectric properties were defined by the bend flexoelectric coefficient $e_{33} = 20$ pC/m, while the splay coefficient e_{11} was set to zero, which reflected the features of mixtures containing the bent-core nematic substance. The presence of ions was neglected, *i.e.* the nematic was treated as perfect insulator. The equilibrium structures of the director field inside the layer were determined by minimization of the free energy counted per unit area of the layer. For this purpose, we used the method which was successfully applied in earlier works [3]. The electric potential distribution $V(y,z)$ in the layer was calculated by resolving the Poisson equation.

3. RESULTS

The results of computations are coherent with earlier data found for non-chiral flexoelectric nematic layers [3]. The two-dimensional deformations arose at some threshold voltage U_1 as shown in Fig. 1 where the maximum polar orientation angle θ_{max} was used as a measure of deformation. The deformation took the form of periodic pattern denoted as the stripes of type 1. Their energy was lower than the energy of simulated one-dimensional deformations.

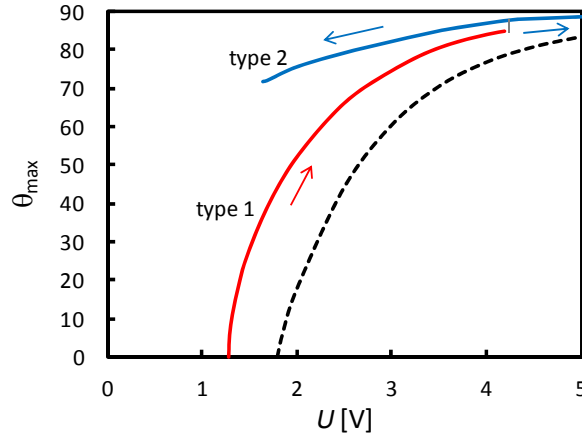


Fig. 1. Maximum polar orientation angle in two-dimensional deformation (solid lines) and in simulated one-dimensional deformation (dashed line) as functions of bias voltage. The arrows show the evolution of deformation during increase and decrease of voltage; $q = 0.065 \mu\text{m}^{-1}$.

The threshold U_1 was smaller than the threshold for uniform deformations. The width of the stripes was initially several times larger than thickness of the layer and decreased with voltage as shown in Fig. 2. Direction of the stripes was determined by the angle ψ ranging between -40° and 0° which varied with voltage (Fig. 3).

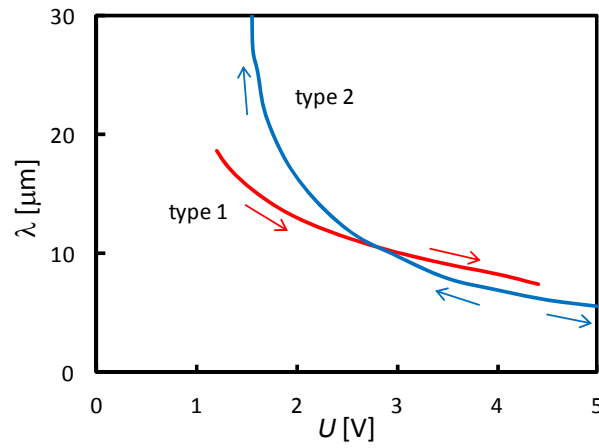


Fig. 2. Space period of the two-dimensional deformation as a function of bias voltage. The arrows show the evolution of deformation during increase and decrease of voltage; $q = 0.196 \mu\text{m}^{-1}$.

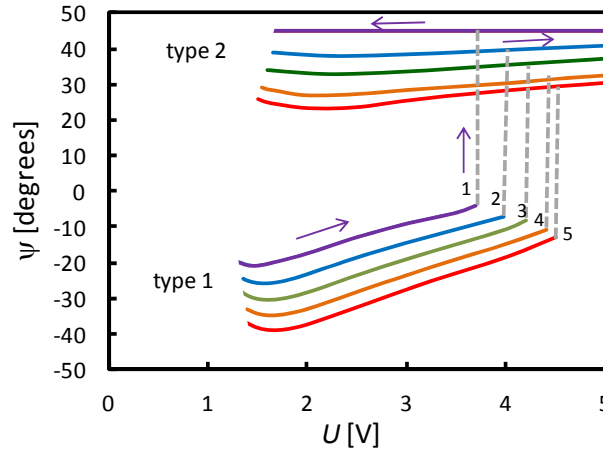


Fig. 3. Direction of the two-dimensional deformations as a function of bias voltage. The arrows show the evolution of deformation during increase and decrease of voltage; 1: $q = 0$; 2: $q = 0.065 \mu\text{m}^{-1}$; 3: $q = 0.131 \mu\text{m}^{-1}$; 4: $q = 0.196 \mu\text{m}^{-1}$; 5: $q = 0.262 \mu\text{m}^{-1}$.

The second type of the periodic deformations, denoted as type 2, appeared discontinuously at some higher threshold U_2 . The type 2 stripes differed from the type 1 in director distribution, in their width and direction. Figure 1 shows that the type 2 deformations developed with increasing voltage and that they were retained if the bias voltage was decreased below U_2 . At some another critical voltage U_3 , the width of the type 2 stripes diverged to infinity leading to one-dimensional deformations (Fig. 2). However, the most peculiar effect revealed during simulations was the significant change of direction of the stripes during transition from type 1 to type 2 presented in Figs. 3 and 4.

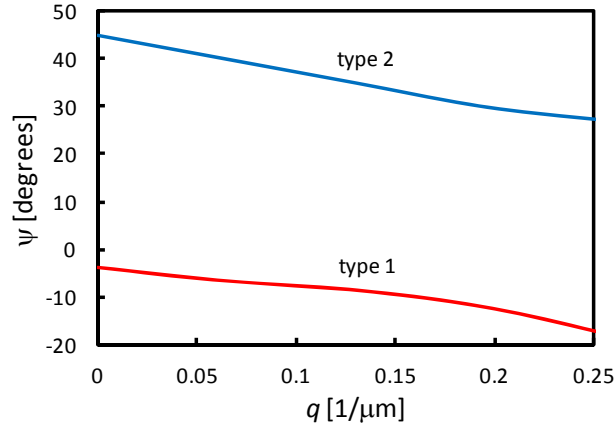


Fig. 4. Directions of the type 1 and type 2 stripes at $U = U_2$.

The scheme of evolution of the stripes described above was found for any value of chirality.

Exemplary director distributions in the cross-sections of single stripes of both types are presented in Fig. 5 for the case of chirality compatible with the 90° twist, $q = 0.262 \mu\text{m}^{-1}$. Slight difference between both distributions can be noticed in the vicinity of the lower electrode where the disclination lines were created. The chirality weakly affected the structure of the deformed layer but it influenced significantly the directions of the periodic patterns. The angle ψ was decreased by c. 15° when the chirality was varied from zero to $q = 0.262 \mu\text{m}^{-1}$ (Fig. 5). In the latter case, the angle ψ for the stripes of type 2 was equal to 45° in agreement with results presented in [3]. The width of the stripes was weakly affected by the chirality. The same concerned the characteristic voltages U_1 , U_2 and U_3 (Fig. 6). The threshold voltage for deformations, U_1 , as well as the value of U_3 were practically constant. The voltage for arising of type 2 deformation, U_2 , slightly increased with chirality.

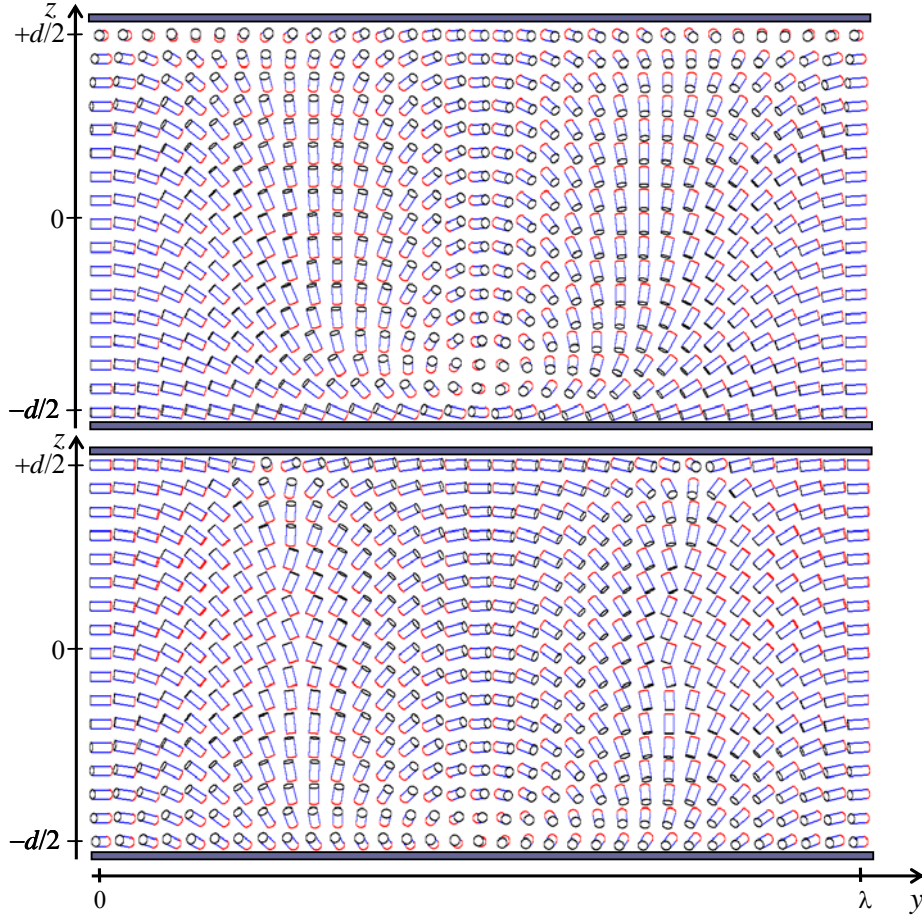


Fig. 5. Director distributions in the cross-sections of single stripes of type 1 (top) and type 2 (bottom), $U = 3$ V, $q = 0.262 \mu\text{m}^{-1}$.

4. SUMMARY

The nematic layer twisted by 90° can be obtained with use of pure nematic as well as with use of substances containing dopants inducing chirality q ranging from zero to $0.262 \mu\text{m}^{-1}$. In each case, the periodic patterns in the form of stripes arose under the action of external electric field. Two types of stripes were observed. It was found that the chirality influences mainly the direction of the periodic patterns whereas the threshold voltage for deformation and the width of the stripes are weakly affected.

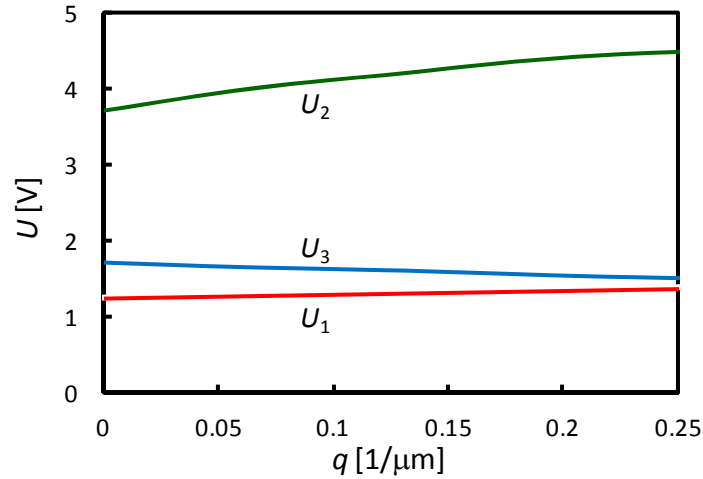


Fig. 6. Characteristic voltages as functions of chirality.

REFERENCES

- [1] D.-K. Yang and S.-T. Wu, *Fundamentals of liquid crystal devices* (John Wiley&Sons Ltd., 2014).
- [2] Umanskil B.A., Chigrinov V.G., Blinov L.M., Podyachev Yu.B. 1981. Flexoelectric effect in twisted liquid-crystal structures. *Sov. Phys. JETP* 54: 694-699.
- [3] Buczkowska M., Derfel G. 2017. Spatially periodic deformations in planar and twisted flexoelectric nematic layers. *Phys. Rev. E* 95: 062705-1 - 062705-8.
- [4] Meyer R.B. 1969. Piezoelectric effects in liquid crystals. *Phys Rev Lett.* 22: 918-921.
- [5] Blinov L.M., *Structure and Properties of Liquid Crystals* (Springer, New York, 2010).
- [6] Derfel G., Buczkowska M. 2016. Two-dimensional deformations in twisted flexoelectric nematic cells. *Sci. Bull. Techn. Univ. Lodz, Physics.* 37: 21-30.
- [7] Harden J., Mbanga B., Eber N., Fodor-Csorba K., Sprunt S., Gleeson J.T., Jakli A. 2006. Giant flexoelectricity of bent-core nematic liquid crystals. *Phys. Rev. Lett.* 97: 157802.
- [8] Jákli A. 2013. Liquid crystals of the twenty-first century – nematic phase of bent-core molecules. *Liq Cryst Rev.* 1: 65-82.
- [9] Derfel G., Buczkowska M. 2015. Macroscopic model formulae describing anisotropic anchoring of nematic liquid crystals on solid substrates. *Sci. Bull. Techn. Univ. Lodz, Physics.* 36: 5-12.

WPLYW CHIRALNOŚCI NA DWUWYMIAROWE ODKSZTAŁCENIA WARSTW NEMATYKÓW FLEKSOELEKTRYCZNYCH

Streszczenie

Dwuwymiarowe deformacje indukowane polem elektrycznym w warstwach ciekłych kryształów nematycznych posiadających właściwości fleksoelektryczne były symulowane numerycznie. Zbadano wpływ chiralnych domieszek na strukturę tych odkształceń i ich rozwój pod wpływem pola elektrycznego. Stwierdzono, że chiralność wpływa głównie na kierunek odkształceń, podczas gdy napięcie progowe na odkształcenie i przestrzenny okres odkształceń słabo zależą od chiralności nematyka.

Stwierdzono, że chiralność wpływa głównie na kierunek odkształceń, podczas gdy jej wpływ na napięcie progowe i na przestrzenny okres odkształceń jest nieznaczny.

**SYLWESTER KANIA^{1,2}, JANUSZ KULIŃSKI²
DOMINIK SIKORSKI³**

¹ Institute of Physics, Lodz University of Technology, ul. Wólczńska 219, 90-924 Łódź, Poland, e-mail: sylwester.kania@p.lodz.pl

² Centre of Mathematics and Physics, Lodz University of Technology, Al. Politechniki 11, 90-924 Łódź, Poland, e-mail: janusz.kulinski@p.lodz.pl

³ Faculty of Material Technologies and Textile Design, Lodz University of Technology, ul. Żeromskiego 116, 90-924 Łódź, Poland, e-mail: dominik.junior@wp.pl

ELECTRICAL AND THERMAL PROPERTIES OF ANTHRAQUINONE LAYERS

Quantum-chemical calculations indicate that the bond lengths in the anthraquinone anthracene backbone are shorter than the corresponding bonds in unsubstituted anthracene. The shape of the frontier molecular orbitals (FMO) indicates the possibility of more efficient electron capture by the anthraquinone molecule than by the anthracene molecule while maintaining stability in the conditions prevailing in electrochemical cells. Differential scanning calorimetry (DSC) studies indicate the temperature stability of anthraquinone above the melting point up to 300 °C. The glass transition is determined at about 100 °C.

Keywords: anthraquinone, differential scanning calorimetry (DSC), DFT calculations.

1. INTRODUCTION

Transport of electric charge through molecular materials is connected with the polarization of the frontier molecular orbitals (FMO). In a crystalline non-organic semiconductor, a high dielectric constant value of about 9 - 13, is connected with strong and effective screening of the charge carrier by a easy and fast readjustment of the distribution of the surrounding space electron density. In organic semiconductor a much smaller value of dielectric constant of about 3 - 4,

enable to create the bonded electron-hole pair named exciton [1]. Charge transport in the organic material can be treated as an addition of the extra electron to the lowest unoccupied molecular orbital (LUMO) or the hole to the highest occupied molecular orbital (HOMO). The hole is used in the meaning of the presence of one electron in the HOMO level instead the two electrons [2]. Charge transport understood in this way requires the appearance of the excited electronic states different from the ground state. Therefore, the conduction process cannot be considered only as a thermal process, or associated only with diffusion or only with electron transport in an electric field, but as a complex physico-chemical process. A characteristic feature of this process is that after the charge transfer process occurs, the molecule is recovered in the ground state. For applications in organic electronics, the thermal resistance of the organic semiconductor layer to Joule-Lenz heat generated during electric conduction is also desirable. For applications, therefore, it is important that the molecule does not undergo dissociation into fragments during the transfer of charge carrier. Therefore, studies on the electrical properties of the material should be associated with studies on thermal properties. An interesting organic compound exhibiting semiconductor properties is anthraquinone. The anthracene skeleton of this molecule is not sensitive to red-ox processes [3]. The only places where the red-ox reaction can occur more easily are oxygen atoms substituted at the position 9 and 10. This fact was used in modern battery design where Al is the metallic anode and anthraquinone is the organic cathode [4]. In such an electrochemical environment, the addition of one electron to each of the oxygen atoms being substituents in the anthraquinone molecule is a reversible reaction.

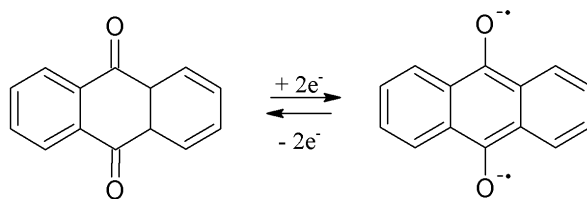


Fig. 1. Addition reaction of two electrons in anthraquinone, under electrochemical stabilization conditions, is a reversible reaction [4].

The problem of chemical resistance to environmental conditions is one of the basic restrictions for practical applications of organic material. However, the above example indicates that the material to be used in the field of electrochemistry and organic electronics additionally should be capable of reversibly subject to red-ox reactions even when excited to higher ionization level.

2. MATERIAL

Anthraquinone represents a low-weight molecular material, which does not crystallize very well [5] *i.e.* in the needle shape from 2-butanone or usually twinned crystals from benzene and toluene [6]. Empirical formula of the molecule is $C_{14}H_8O_2$, molecular weight 208.22. The molecule is planar, all of the hydrogen atoms are placed in the anthracene skeleton plane [7]. The earlier X-ray diffraction studies on anthraquinone [7] assigned the monoclinic crystal system with space group $P2_1/a$ and lattice constants $a = 15.810 \pm 0.015 \text{ \AA}$, $b = 3.942 \pm 0.005 \text{ \AA}$, $c = 7.865 \pm 0.010 \text{ \AA}$ and $\beta = 102^\circ 43' \pm 2'$ and unit cell volume 477.8 \AA^3 . More recent studies [5,6] have indicated space group $P2_1/c$ with the lattice parameters shown in Table 1 [6]. The unit cell volume determined from this measurements is $480.21(7) \text{ \AA}^3$ [6] in temperature of 296 K. To determine the effect of the presence of two substituents in Table 1, in addition to the properties of two described anthraquinone crystal structures, the properties of two anthracene crystal structures are also given [8,9]. Anthracene crystallizing in the monoclinic crystal system has the unit cell volume equal to $473.66(16) \text{ \AA}^3$ [9] close to that of anthraquinone unit cell. However the lattice constants of the two compounds are significantly different.

Table 1

The parameters of the monoclinic crystal structures of anthraquinone [6] at 296 K and anthracene [8, 9] at 293 K and their molecular dipole moments [10]

Compound	Space group	Lattice constant, [Å]	Lattice angle, β [degrees]	Dipole moment, [D]
Anthraquinone ($C_{14}H_8O_2$) [6]	$C_{2h}^5(P2_1/c)$	$a_0 = 7.8684(5)$ $b_0 = 3.9634(3)$ $c_0 = 15.7839(13)$	102.687(6)	0,6 (in benzene)
Anthracene ($C_{14}H_{10}$) [9]	$C_{2h}^5(P2_1/c)$	$a_0 = 11.166(2)$ $b_0 = 6.021(1)$ $c_0 = 8.553(2)$	124.54(3)	
Anthracene ($C_{14}H_{10}$) [8]	$C_{2h}^5(P2_1/c)$	$a_0 = 8.553$ $b_0 = 6.021$ $c_0 = 18.849$	102.59(3)	

The values given in the Table 1 and cited in the text above from [7] indicate significant difficulties in determining the actual crystal structure of both anthracene and its anthraquinone derivative. Therefore, for a more accurate analysis of the properties the solid state and the properties of the molecule itself, it is beneficial to use quantum-chemical calculations [5]. The best consistency of

the calculation results with the X-ray structural characterization in the case of anthraquinone is obtained when density functional theory (DFT) calculations on the B3LYP/6-311 level of theory are performed [5]. Also our previous calculations [11,12] indicated that DFT calculations can be used to determine the energy distribution and the spatial distribution of both the molecule itself and the electrical properties associated with the anthraquinone crystal lattice cell.

3. QUANTUM-CHEMICAL CALCULATION

The calculations in the gas phase were carried out with use GAUSSIAN 09 program [13] with use of DFT calculations in the 6-311+g(d,p) level of theory. The structure parameters of anthraquinone molecule being in the neutral, kation and anion state were determined. Optimization of the molecule structure of anthraquinone allowed us to determine the values of bond length in the anthraquinone molecule. The electrical properties in the volume of the anthraquinone are associated with both the crystal packing of the molecules and the structure itself and only with the structure of the molecule itself. The question therefore arises whether the properties of the material are determined by the skeleton properties itself, or whether two oxygen substitution in the positions 9 and 10 has a significant impact.

3.1. Calculations of anthraquinone molecule

The anthraquinone molecule consists of a rigid skeleton of anthracene, which is a linear system of three benzene rings substituted in the middle ring symmetrically with two oxygen atoms.

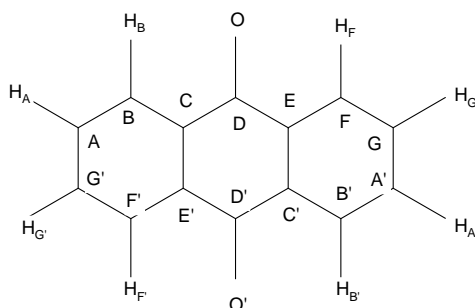


Fig. 2. Anthraquinone molecule. The marking of atoms takes into account the symmetry of the molecule.

Quantum-chemical calculations indicate that substitution of the anthracene skeleton with two oxygen atoms significantly changes the length of corresponding bonds in both the anthracene and anthraquinone molecules (Fig. 2). The calculated differences of bond lengths in gas phase for anthracene and anthraquinone in the case of chemically equivalent bonds DE and D'C', EF and C'B' as well as FG and B'A' are +0,094 Å (6.7%), -0.031 Å (2.1%) and +0.022 Å (1,6%), respectively (Table 2). There is observed that the length of pair of bonds DE and D'C' in anthracene are nearly equal to the pair of bonds FG and B'A' of anthraquinone, and the length of pair of bonds DE and D'C' in anthraquinone are nearly equal to the pair of bonds FG and B'A' of anthracene. It is well known that the bond energy in organic chemistry depends on the bond length: the shorter the bond, the more energetic it is. This is associated with the trend for stabilization energy in the manner that when the shorter bond is in the benzene ring then the greater stabilization energy is and consecutively the more aromatic benzene ring will be [14]. In general, the local aromaticity of the oligoacene molecule increases steadily from the peripheral to the central ring [15]. This tendency is clearly seen for anthracene. For anthraquinone the greater aromaticity can be connected with peripheral ring and the lower one with central ring.

Table 2
Equivalence of bonds in the structure of molecule anthracene and molecule anthraquinone (calculation made with DFT B3LYP/6-311++G(d,p)). Identification of bonds as in Fig. 2, and length in Å

	Bond	Bond length gas phase anthracene	Bond length gas phase anthraquinone	Bond length solid phase anthraquinone, from X-ray diffraction crystallography [5]	Difference of bond length, 4-3
1	2	3	4	5	6
bonds chemically equivalent	DE and D'C'	1.3989	1.4924	1.487(2) and 1.481(2)	+0.094
	EF and C'B'	1.4293	1.3984	1.393(2) and 1.395(2)	-0.031
	FG and B'A'	1.3674	1.3897	1.381(2) and 1.379(2)	+0.022
bonds chemically different	FG and A'G	1.3674 and 1.4250	1.3897 and 1.3978	1.381(2) and 1.377(3)	
	EF and EC'	1.4293 and 1.4427	1.3984 and 1.4064	1.393(2) and 1.398(2)	
	EC' and GA'	1.4427 and 1.4250	1.4064 and 1.3978	1.398(2) and 1.377(3)	

When examining the case of pairs of chemically different bonds, *i.e.* FG and A'G, EF and EC' as well as EC' and GA', the greater differentiation in the case of anthracene than for anthraquinone molecules is seen.

The data given in Table 2, Table 3 and Table 4 indicate that changes in the length of bonds in the molecule are reflected in the image of the electron density distribution of the molecule. It is clearly visible a different picture of external frontier molecular orbitals (FMO), *i.e.* HOMO and LUMO orbitals for both anthracene and anthraquinone molecules.

Table 3

Comparison of the shape of anthracene and anthraquinone frontier molecular orbitals (FMO) important for conduction of holes

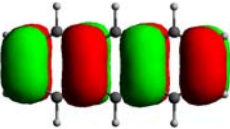
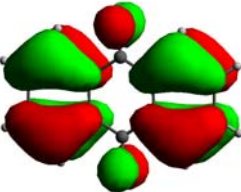
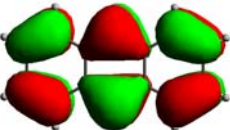

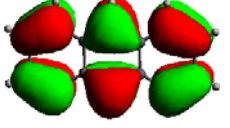
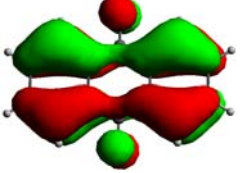
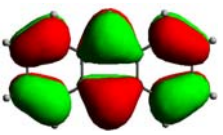
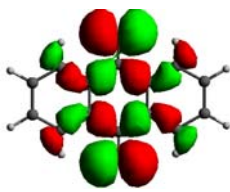
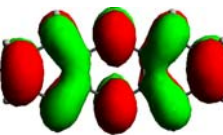
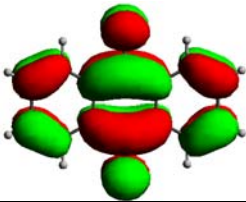
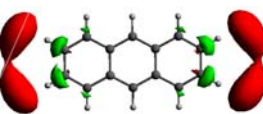
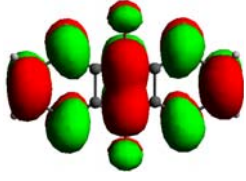
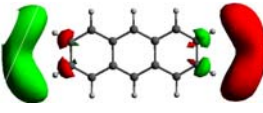
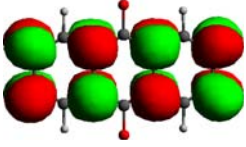
FMO	Charge of the molecule	Anthracene	Anthraquinone
HOMO-1	0 neutral		
HOMO	0 neutral		
HOMO	+1 cation		

Table 4

Comparison of the shape of anthracene and anthraquinone frontier molecular orbitals (FMO) important for electrochemical stabilization in the conditions when is need to connect one or two extra electrons to the molecule

FMO	Charge of the molecule	Anthracene	Anthraquinone
HOMO-1	-1 anion		
HOMO	-1 anion		
LUMO	-1 anion		
LUMO+1	-1 anion		

3.2. Discussion

The results of calculations for hole conductivity (Table 3) indicate that hole conductivity associated with the transfer of electrons between external FMO orbitals, *i.e.* HOMO, HOMO-1 is possible for both anthraquinone and anthracene. The anthraquinone molecule has a spatial distribution of HOMO

orbitals such that conduction of holes can occur even when ionising this molecule to the charge state of +1. This would allow the use of anthraquinone for active layers under conditions of positive ionization of molecules, *e.g.* under conditions existing in electrochemical cells.

When anthraquinone molecule is an anion, it has such a spatial distribution of FMO orbitals (Table 4) that allows conduction of electrons.

Comparison of the shape of the outer orbitals (FMO) of both anthraquinone and anthracene molecules in the anion state, important for electrochemical stability, *i.e.* under the conditions when of one or two electron must be connected to the molecule (Table 2), indicates that under these conditions anthraquinone is stable. Molecule of anthracene in this conditions has no possibility to hold the electron in the benzene rings of the skeleton.

4. MEASUREMENTS AND DISCUSSION

4.1. DSC measurements

To determine the stability of the compound at melting temperature we used the measurement method of scanning calorimetry – differential scanning calorimetry (DSC). The DSC method allows to made simultaneous measurement of both the temperature and heat flow. They are recorded as a function of time and temperature. The difference in the amount of heat required to increase the temperature of the sample crucible and reference crucible is recorded. DSC measurement allows qualitative and quantitative determination of physical and chemical changes that are associated with endothermic and exothermic processes, as well as changes in heat capacity.

The measurement was made using a TA Instruments Universal Analysis Q2000 computer controlled research-grade DSC device for temperature and heat flow regulation. The measuring system diagram is presented in Fig. 3.

The DSC technique, due to the automation of its precision measurement, does not require the use of a large number of samples to perform the measurement. Thermal analysis is performed automatically on small samples. The measurements were made with anthraquinone with purity grade > 99% (HPLC) from Fluka with flash point 185°C and melting point in the range of 283-287°C.

DSC curve is presented in Fig. 4. The sample mass was 11.260 mg, and the measurement was made in the ambient of nitrogen gas. Heating rate was 0.35°C/min, start temperature was 25°C and final temperature 300°C.

Melting temperature of anthraquinone was determined to be $T_c = 284.56^\circ\text{C}$ (Fig. 4b). Glass transition point was observed in the region where the inflection point of thermal curve was registered, *i.e.* at $T_g \approx 100^\circ\text{C}$ (Fig. 4a). The examined material did not decompose after passing through the melting point.

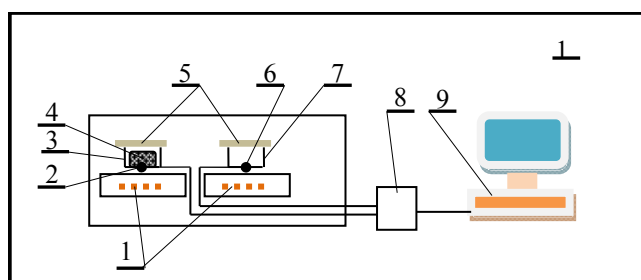


Fig. 3. Experimental scheme of DSC apparatus, 1 – heaters, 2 – measuring thermocouple, 3 – crucible with a sample, 4 – sample, 5 – covers, 6 – reference thermocouple, 7 – reference crucible, 8 – interface, 9 – computer reading the temperature and regulating heat flow.

4.2. Discussion

The obtained melting temperature of anthraquinone $T_c = 284.56^\circ\text{C}$. is consistent with the results of Fu *et al.* [5], where this value was set at $T_c = 284.8^\circ\text{C}$. During melting, anthraquinone does not decompose. The fact Interesting from the point of view of organic electronics applications is that the glass transition temperature for anthraquinone appears about 100°C , *i.e.* above the operating temperatures of electronic devices used in commercial applications at room temperatures.

5. CONCLUSIONS

During transport of charge carriers through the material, the charge transfer through the molecule must occur. This charge transfer through molecule can be interpreted as occurrence of red-ox processes. Therefore, it is important that the molecule does not dissociate and the electron transfer reactions should be reversible. These requirements are met by the anthraquinone molecule. The stability of the anthraquinone molecule for applications of organic electronics is a compromise between the required stability of the molecule and the required electron transfer reactions. These conditions are forced by the need to meet specific requirements resulting from the use of an electronic device using

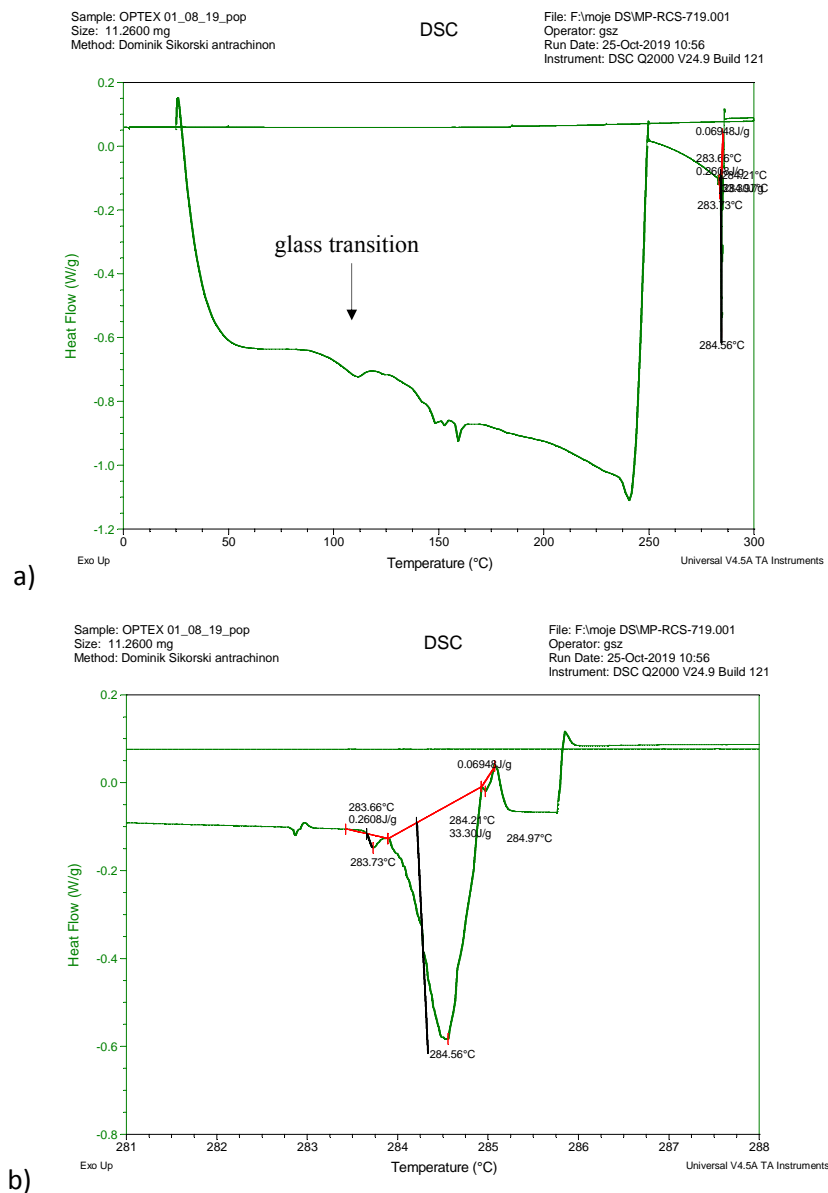


Fig. 4. Determination of antrachinone melting point by DSC method, a) thermogram for the entire measuring range (visible transition associated with the transition of glass transition at a temperature of about 100°C), b) enlarged area near the melting point.

anthraquinone as an active material. Anthraquinone can be used as an active substance working in solid state electronics devices because it is not subject to thermodynamic changes of the structure up to about 100°C, where it is subject to glass transition. In the DSC measurement range, *i.e.* up to 300°C, it is not dissociated into fragments.

Quantum-chemical calculations indicate that the bond lengths in the anthracene skeleton of anthraquinone molecule are shorter than the corresponding bonds in non-substituted anthracene. The shape of external orbitals (FMO) indicates the possibility of effective electron capture by the anthraquinone molecule while maintaining stability in the conditions existing in electrochemical cells. Anthracene molecule does not meet such conditions. DSC studies indicate the chemical stability of anthraquinone above the melting point. Electronic properties including the shape of FMO orbitals and temperature resistance of anthraquinone molecules allow to treat this material as having potential for use as active material in electronics.

6. ACKNOWLEDGEMENTS

The DSC measurements were made in the Institute of Material Science of Textiles and Polymer Composites at Faculty of Material Technologies and Textile Design, Lodz University of Technology.

The quantum-chemical calculations mentioned in this paper are performed using the PLATON project's infrastructure at Lodz University of Technology Computer Centre.

REFERENCES

- [1] Yamagata H., Norton J., Hontz E., Olivier Y., Beljonne D., Brédas J. L., Silbey R. J., Spano F.C. 2011. The nature of singlet excitons in oligoacene molecular crystals. *J. chem. phys.* 134: 204703-1-204703-1. <http://dx.doi.org/10.1063/1.3590871>
- [2] Köhler A., Bässler H. 2011. What controls triplet exciton transfer in organic semiconductors?. *J. mater. chem.* 21: 4003-4011. <https://doi.org/10.1039/c0jm02886j>
- [3] Phillips M. 1929. The chemistry of anthraquinone. *Chem. Rev.* 6: 1, 157-174. <https://doi.org/10.1021/cr60021a007>
- [4] Bitenc J., Lindahl N., Vizintin A., Abdelhamid M. E., Dominko R., Johansson P. 2020. Concept and electrochemical mechanism of an Al metal anode – organic cathode battery. *Energy Storage Materials* 24: 379-383. <https://doi.org/10.1016/j.ensm.2019.07.033>

- [5] Slouf M. 2002. Determination of net atomic charges in anthraquinone by means of 5-h X-ray diffraction experiment. *J. mol. struct.* 611: 1-3, 139-146. [https://doi.org/10.1016/S0022-2860\(02\)00060-1](https://doi.org/10.1016/S0022-2860(02)00060-1)
- [6] Fu Y., Brock C. P. 1998. Temperature dependence of the rigid-body motion of anthraquinone. *Acta Cryst. B54*: 308-315. <https://doi.org/10.1107/S0108768197013414>
- [7] Murty B.V.R. 1960. Refinement of the structure of anthraquinone. *Z. Kristallogr.* 113: 445-465. http://rruff.info/uploads/ZK113_445.pdf
- [8] Marciniak B., Pavlyuk V. 2010. Crystal Structure of a Metastable Anthracene Modification, Grown from the Vapor Phase. *Mol. cryst. liq. cryst.* 373:1, 237-250. <https://doi.org/10.1080/10587250210538>
- [9] Marciniak B., Różycka-Sokołowska E., Balińska A., Davydov W., Pawliuk W. 2000. Crystal structure and morphology of vapour grown anthracene crystals. *Visnyk lviv univ. ser. phys.* 33: 277-282.
- [10] Landolt-Börnstein. 1971. *Zahlenwerte und Funktionen aus Naturwissenschaften und Technik*, Berlin: Springer Verlag.
- [11] Kania S., Kościelniak-Mucha B., Kuliński J., Słoma P. 2016. The effect of symmetry of a molecule electronic density on the dipole moment of unit cell and hole conductivity of thin polycrystalline films of anthrone and anthraquinone. *Sci. Bull. Techn. Univ. Lodz, Physics*, 37: 49-64. <https://doi.org/10.34658/physics.2016.37.49-64>
- [12] Kania S., Kościelniak-Mucha B., Kuliński J., Słoma P. 2015. Effect of molecule dipole moment on hole conductivity of polycrystalline anthrone and anthrachinone layers. *Sci. Bull. Techn. Univ. Lodz, Physics*, 36: 13-25. <http://cybra.lodz.pl/dlibra/publication/17133/edition/13805/content>
- [13] Gaussian 09, Revision A.02. 2009. Frisch M.J., Trucks G.W., Schlegel H.B., Scuseria G.E., Robb M.A., Cheeseman J.R., Scalmani G., Barone V., Mennucci B., Petersson G.A., Nakatsuji H., Caricato M., Li X., Hratchian H.P., Izmaylov A.F., Bloino J., Zheng G., Sonnenberg J.L., Hada M., Ehara M., Toyota K., Fukuda R., Hasegawa J., Ishida M., Nakajima T., Honda Y., Kitao O., Nakai H., Vreven T., Montgomery J.A., Peralta Jr., J.E., Ogliaro F., Bearpark M., Heyd J. J., Brothers E., Kudin K.N., Staroverov V.N., Kobayashi R., Normand J., Raghavachari K., Rendell A., Burant J.C., Iyengar S.S., Tomasi J., Cossi M., Rega N., Millam J.M., Klene M., Knox J.E., Cross J.B., Bakken V., Adamo C., Jaramillo J., Gomperts R., Stratmann R.E., Yazyev O., Austin A.J., Cammi R., Pomelli C., Ochterski J.W., Martin R.L., Morokuma K., Zakrzewski V.G., Voth G.A., Salvador P., Dannenberg J.J., Dapprich S., Daniels A.D., Farkas O., Foresman J.B., Ortiz J.V., Cioslowski J., Fox D.J., Wallingford CT: Gaussian, Inc.
- [14] Krygowski T.M., Cyrański M.K. 2001. Structural aspects of aromaticity. *Chem. Rev.* 101: 1385-1419. <https://doi.org/10.1021/cr990326u>
- [15] Portella G., Poater J., Bofill J.M., Alemany P., Sola M. 2004. Local Aromaticity of [n]Acenes, [n]Phenacenes, and [n]Helicenes (n = 1-9). *J. org. chem.* 70: 7, 2509-2521. <https://pubs.acs.org/doi/10.1021/jo0480388>

WŁASNOŚCI ELEKTRYCZNE I TERMICZNE WARSTW ANTRACHINONU

Streszczenie

Obliczenia kwantowo-chemiczne wskazują, że długości wiązań w szkielecie antracenowym antrachinonu w zewnętrznym pierścieniu benzenowym są krótsze niż odpowiadające im wiązania w niepodstawionym antracenie. Świadczy to o zwiększeniu energii rezonansu w zewnętrznych pierścieniach benzenowych cząsteczki antrachinonu. Kształt orbitali zewnętrznych (FMO) wskazuje na możliwość bardziej efektywnego przejmowania elektronów przez cząsteczkę antrachinonu niż przez cząsteczkę antracenu z zachowaniem stabilności w warunkach panujących w komórkach elektrochemicznych. Badania DSC wskazują na stabilność chemiczną antrachinonu powyżej temperatury topnienia aż do 300°C. Antrachinon w pobliżu temperatury 100°C wykazuje przemianę zeszklenia, poniżej tej temperatury nie wykazuje przemian fazowych. Własności elektryczne i termiczne antrachinonu wskazują na duży potencjał tego związku dla zastosowań w elektronice organicznej.

**SYLWESTER KANIA^{1,2}, BARBARA KOŚCIELNIAK-MUCHA²
JANUSZ KULIŃSKI², PIOTR SŁOMA²
KRZYSZTOF WOJCIECHOWSKI²**

¹ Institute of Physics, Lodz University of Technology, ul. Wólczańska 219, 90-924 Łódź, Poland, e-mail: if@p.lodz.pl

² Centre of Mathematics and Physics, Lodz University of Technology, al. Politechniki 11, 90-924 Łódź, Poland, e-mail cmf.adm@p.lodz.pl

POLARIZATION OF ORGANIC AROMATIC MOLECULE IN ANIONIC AND CATIONIC STATE

The modification of electron states and the change in the geometry of the structure of molecule during hopping transport of charge carriers depends on the symmetry of the molecule. During electric transport the molecule reversibly transforms from neutral state to cation when hole conductivity occurs or to anion when electron conductivity occurs. The energies of orbitals HOMO and HOMO-1 of anthrone and anthrachinone are always negative, what allows for holes transport. Positive energies of LUMO and LUMO+1 orbitals of anion of anthrone and anthraquinone in structure of anion or neutral molecule make electron transport difficult.

Keywords: DFT, anthraquinone, anthrone, charge transport.

1. INTRODUCTION

The results of quantum-chemical calculations allow to specify the hopping conduction parameters at the molecular level [1, 2, 3]. Conduction in a high-resistance material occurs in two stages. The first stage is the takeover of a charge carrier by the molecule in the form of the entire electron or entire hole. The second stage is transferring a single electron between neighbouring molecules [4, 5, 6]. This process should be independent of the existence of bonds between molecules of organic material and it cannot be carried out in such a way that solid phase damage would occur. Maintaining stability of solid phase in the organic semiconductor under equilibrium conditions is possible due to the

existence of van der Waals or London dispersion forces [7] appearing when the electron density fluctuations of neighbouring molecules occur. The lack of charge transfer of the value of the charge of the whole electron from one molecule to another is a special feature of such binding interactions. Even if the above-mentioned interactions are strong, they are not accompanied by the transfer of charge equal or greater than the charge of one electron from one molecule to another. There is also no strong localization of an electron pair between neighbouring molecules what is a special property of covalent bond. The strength of intermolecular interactions is significantly determined by the distance between the centers of mass (centroids) of the molecules, but the twisting of the planes of molecules relative to each other also plays an important role. Possibility of occurrence of favourable π -stacking interactions between molecules for electric conduction depends on the orientation of molecules. At equilibrium, the distance between centroids of the organic molecules forming the crystalline solid phase is quite significant, and in the case of anthracene and its derivatives is of the order of 4 Å. When the distance between the centers of the molecules is above about 8 Å then the molecules practically do not interact and the molecular orbitals do not contribute to conductivity [5]. The lack of charge transfer between molecules in dispersion interactions allows treating these interactions almost as a kind of physical adsorption or chemisorption. There is no spontaneous unilateral flow of electrons between adjacent molecules under equilibrium conditions therefore, an effective equilibrium for red-ox reactions connected with electron taking over by molecules is observed. However, polarization by an external electric field causes current flow through layers made of organic molecules which involves the molecules to uptake the electrons. Thus, there must be a step when the next molecule takes over the entire electron previously released from the preceding molecule during the charge carrier transfer process.

This electron exchange between neighbouring molecules can be considered as a chemical reaction. Marcus-Hush theory [4] enables to understand the process of conduction as a red-ox reaction string to which organic matter molecules are subjected while transferring charge carriers occurs. This theory was used to describe hopping conduction in organic materials in the 1990s. Total charge of a molecule changes during the process of charge transfer. Molecule transferring an electron as a negative charge carrier becomes an anion for a short time, while a molecule carrying a positive charge carrier (hole) becomes a cation for a short time. The molecule returns to the neutral state after completing such a red-ox reaction which is the special feature of this process. The molecule does not dissociate into fragments and has the same properties as before the process of taking charge and transferring the charge carrier. The energy effect associated with such a process can be calculated as reorganization energy [1, 5].

The value of the reorganization energy for conduction of holes is λ_+

$$\lambda_+ = \lambda_c + \lambda_n = (E_{kn} - E_{kk}) + (E_{nk} + E_{nn}), \quad (1)$$

where λ_c is the energy necessary for the reorganization of the neutral geometry of molecule to the cation geometry during electron removal. The symbol λ_n denotes the energy necessary for the reorganization to change the cation geometry again to the neutral geometry when attached electron from the neighbouring molecule.

Therefore, to determine the reorganization energy for hole conductivity, the total energy for the molecule in the following states should be determined:

- E_{nn} is optimized state of the neutral molecule,
- E_{kk} is optimized state of the molecule being a cationic radical,
- E_{kn} is optimized state of the molecule being a cation in the structure of a neutral molecule,
- E_{nk} is optimized state of the neutral molecule in the cation structure.

Similar calculations are carried out in the case of reorganization energy calculation, λ_- for electron transport

$$\lambda_- = \lambda_c + \lambda_n = (E_{an} - E_{aa}) + (E_{na} + E_{nn}), \quad (2)$$

Here, λ_- is calculated as the sum of λ_c for the energy necessary to reorganize the geometry of the neutral molecule to the anion geometry when attaching the electron, and λ_n for the energy necessary for the reorganization to change the geometry of the anion again to the geometry of the neutral molecule when the electron is donated to the neighbouring molecule.

Therefore, to determine the reorganization energy for electron transport, the total energy for a molecule in the following states should be determined as follows:

- E_{nn} is optimized state of the neutral molecule,
- E_{aa} is optimized state of the molecule being an anionic radical,
- E_{an} is optimized state of the molecule being anion in the structure of the neutral molecule,
- E_{na} is optimized state of the neutral molecule in the anion structure.

Experimental results revealed that the mobilities of charge carriers are different in the case of conduction of layers of two anthracene derivatives. This difference is observed for both crystalline and amorphous samples [8]. It was shown in our previous work [1] that this difference has its origin in the existence of a constant dipole moment in anthron molecules and lack of it in anthraquinone molecules. Analysis of solid phase X-ray studies [4, 7] and our quantum mechanical calculations carried out for both considered molecules [9]

proved that the change in aromatic stabilization energy, calculated relative to unsubstituted anthracene, is practically the same and amounts to approx. 1%. This feature is observed despite of the fact that the central benzene ring of anthrone molecule is substituted with one ketone group and for anthraquinone molecule central benzene ring is substituted symmetrically with two ketone groups. This is accompanied by an almost equal change in the length of bonds between carbon atoms in the side and the middle rings, which is about 6.4% for both molecules under study. Thus, there is no noticeable steric effect associated with symmetrical or asymmetrical substitution of the middle anthracene ring with one or two ketone groups on reorganization energy.

The question arises here whether the polarity of the molecule has an impact on the stability of the excited states of the cation and anion and enables hole or electron transport.

We want to find answer to this question calculating the states of external orbitals (FMO) of the two molecules under consideration. We carry out analysis of the states of molecules that are used to define the reorganization energy defined by formula (1) for transport of holes and formula (2) for electron transport.

2. CALCULATION RESULTS AND DISCUSSION

The "four-point" [1, 5] method (Eqs. (1) and (2)) was used to calculate the reorganization energy. DFT calculations were carried out using the Gaussian 09 program [10] at the level of theory B3LYP/6-311+G(d, p). The calculations in the scope of the "four-point" method required the calculation of the structure of the molecule in the cation, anion and in the neutral state. They were performed for molecules in the gas phase. The choice of calculations in the gas phase is associated with the observation that the strong localization of charge carriers on molecules in oligoacene derivatives causes that the electronic states of the molecule are similar in the gas phase and in the solid phase [11]. The shift caused by the presence of the crystal field is almost constant for all external orbitals given molecule [12]. The differences in the energy of external orbitals and not their absolute values are important for our considerations.

An interesting problem is the possibility of realizing a stable molecule in the cation or anion state. In order to answer this question, the calculation of the energy value of the levels HOMO, HOMO-1, LUMO and LUMO+1 is required. LUMO levels are important for electron conduction while HOMO levels are important for conduction of holes. The molecule is not stable in the gas phase when the obtained energy values of the orbital are non-negative. The additional

multi-body interactions that counteract the destruction of the solid phase caused by the flow of the charge carrier through the molecule appear in the presence of particles in the solid phase.

The results of quantum-chemical calculations obtained by us allow for preliminary determination of cation and anion stability. Tables 1 and 2 show the results of calculations for the anthraquinone and the anthron molecules, respectively. Both molecules are derivatives of anthracene, and they crystallize in almost the same crystal structure with similar lattice constants [13, 14]. The results for the unsubstituted anthracene molecule are shown in Table 3 for comparison.

Table 1
Calculated electronic properties of molecule of anthraquinone during transfer of charge carrier

	1	2	3	4	5	6	7	8
			[D]	[eV]	[eV]	[eV]	[eV]	[eV]
cation in cation structure	+1	doublet	0.0033	-11.9545	-11.9376	-7.7414	-6.2945	4.196
cation in neutral structure	+1	doublet	0.0003	-11.8503	-11.7825	-7.9882	-6.3789	3.794
neutral in cation structure	0	singlet	0.0003	-7.5898	-7.3144	-3.1421	-2.0180	4.172
neutral in neutral structure	0	singlet	0.0003	-7.5786	-7.3969	-3.1865	-2.0583	4.210
neutral in anion structure	0	singlet	0.0002	-7.5814	-7.4741	-3.5329	-2.1062	3.941
anion in neutral structure	-1	doublet	0.0003	-2.7900	-0.0185	1.9124	2.2757	1.930
anion in anion structure	-1	doublet	0.0001	-2.8806	-0.3777	1.8607	2.2640	2.238

1 - charge, 2 - spin, 3 - dipole moment, 4 - HOMO-1, 5 - HOMO, 6 - LUMO, 7 - LUMO+1, 8 - E_g .

Table 2
Calculated electronic properties of molecule of anthrone during transfer of charge carrier

	1	2	3	4	5	6	7	8
			[D]	[eV]	[eV]	[eV]	[eV]	[eV]
cation in cation structure	1	doublet	4.7756	-11.4843	-11.1246	-6.2806	-5.5054	4.843
cation in neutral structure	1	doublet	4.7156	-11.5403	-11.0816	-6.3318	-5.3854	4.750
neutral in cation structure	0	singlet	3.8761	-7.0818	-7.0042	-2.1004	-1.0653	4.904
neutral in neutral structure	0	singlet	3.8667	-7.0426	-7.2649	-2.1437	-0.9442	5.121
neutral in anion structure	0	singlet	4.0854	-7.1332	-7.0290	-2.5007	-0.8898	4.528
anion in neutral structure	-1	doublet	4.6776	-2.2101	0.9891	2.2601	2.3587	1.271
anion in anion structure	-1	doublet	4.8151	-2.2422	0.6059	2.2490	2.3467	1.643

1 - charge, 2 - spin, 3 - dipole moment, 4 - HOMO-1, 5 - HOMO, 6 - LUMO, 7 - LUMO+1, 8 - E_g .

In the case of hole conductivity, both HOMO and HOMO-1 levels for anthraquinone, anthron and anthracene are significantly below the vacuum level. Thus, we can conclude that conduction of holes is always possible both for anthraquinone and for anthrone. The energy values of the LUMO and LUMO+1 levels are decisive for electron conduction. For the molecule in the neutral state in the neutral structure as well neutral in the anion structure for both

anthraquinone and anthron molecules the energies of the LUMO and LUMO+1 levels are negative. However, the transition of the molecule to the anion structure (in the -1 charge state) leads to positive high energy values (above 1.8 eV) of the LUMO and LUMO+1 orbitals. Even if the energy shift caused by the presence of a crystal field is taken into account, which according to some estimates for anthracene derivatives may have a value of even 1.7 eV [12], the energy values of LUMO orbitals do not allow maintaining anion stability in solid state. This means that the implementation of effective transport of negative carriers in anthraquinone and anthron is difficult. Moreover, in the case of anthrone, the positive energy of its HOMO level in the anion state indicates that obtaining a stable anion of the anthrone is difficult.

Table 3
Calculated electronic properties of molecule of anthracene during transfer of charge carrier

	1	2	3	4	5	6	7	8
			[D]	[eV]	[eV]	[eV]	[eV]	[eV]
cation in cation structure	1	doublet	0	-11.1836	-10.1681	-6.7775	-4.9838	3.390
cation in neutral structure	1	doublet	0	-11.1330	-9.4758	-6.6254	-5.0630	2.850
neutral in cation structure	0	singlet	0	-6.8676	-5.4415	-2.1568	-0.6900	3.284
neutral in neutral structure	0	singlet	0	-6.7988	-5.5764	-2.0240	-0.7483	3.552
neutral in anion structure	0	singlet	0	-6.8856	-5.4564	-2.2120	-0.7581	3.236
anion in neutral structure	-1	doublet	0	-1.5913	1.0294	2.4330	2.4751	1.403
anion in anion structure	-1	doublet	0	-1.4909	0.8297	2.4251	2.4624	1.595

1 - charge, 2 - spin, 3 - dipole moment, 4 - HOMO-1, 5 - HOMO, 6 - LUMO, 7 - LUMO+1, 8 - E_g

Despite the similarity of the molecules and the structures in which they crystallize, there is a significant difference in the value of the energy gap E_g between molecules under consideration. Anthrone having a permanent dipole moment has the value of the energy gap clearly higher than anthraquinone and anthracene.

3. CONCLUSIONS

The results of calculation clearly indicate the high stability of the anthraquinone and the anthrone cations. The conductivity of holes in solid phase is possible for both materials in this situation.

A high positive value of LUMO and LUMO+1 levels for anthraquinone above 1.8 eV does not allow for stable electron conduction in anthraquinone solid phase. However, the negative value of the HOMO level for the anion

allows the molecule to move through the solid phase to the basic level of the anion, in the ionization state +1. This allows application of anthraquinone in the form of a solid phase for the needs of technology used in electrochemical environment.

The high positive value of HOMO, LUMO and LUMO+1 levels for the anthrone does not allow the anthrone to be obtained in a stable anion state. This makes effective electron transport for applications in organic electronics more difficult to accomplish. It should be noted, however, that the properties of anthrone anion are more favourable for applications than the properties of unsubstituted anthracene anion.

Despite the similarity of the molecules and structures in which they crystallize, there is a significant difference in the value of the energy gap E_g between anthrone, anthraquinone and anthracene.

The obtained results indicate other areas of possible applications of anthraquinone and anthrone in organic electronics.

The high value of the forbidden gap can be beneficial for the use of both materials for the production of active layers in solar cells, where high resistance is required due to the need to separate generated charges.

REFERENCES

- [1] Oberhofer H., Reuter K., Blumberger J. 2017. Charge transport in molecular materials: an assessment of computational methods. *Chem. Rev.* 117: 10319-10357. <https://doi.org/10.1021/acs.chemrev.7b00086>
- [2] Kukhta A.V., Kukhta I.N., Kukhta N.A., Neyra O.L., Meza E. 2008. DFT study of the electronic structure of anthracene derivatives in their neutral, anion and cation forms. *J. Phys. B: At. Mol. Opt. Phys.* 41: 20, 205701. <https://doi.org/10.1088/0953-4075/41/20/205701>
- [3] Wen S.-H., Li A., Song J., Deng W.-Q., Han K.-L., Goddard III W.A. 2009. First-principles investigation of anisotropic hole mobilities in organic semiconductors. *J. Phys. Chem. B* 113: 8813-8819. <https://pubs.acs.org/doi/10.1021/jp900512s>
- [4] Marcus R.A. 2000. Tutorial on rate constants and reorganization energies. *J. Electroanal. Chem.* 483: 1-2, 2-6. [https://doi.org/10.1016/S0022-0728\(00\)00011-5](https://doi.org/10.1016/S0022-0728(00)00011-5)
- [5] Datta A., Mohakud S., Pati S.K. 2007. Electron and hole mobilities in polymorphs of benzene and naphthalene: role of intermolecular interactions. *J. Chem. Phys.* 126: 144710-1-144710-6. <https://doi.org/10.1063/1.2721530>
- [6] Marcus R.J. 1993. Electron transfer reactions in chemistry. Theory and experiment. *Rev. mod. phys.* 65: 3, 599-610. <https://doi.org/10.1103/RevModPhys.65.599>
- [7] Ehrlich S., Moellmann J., Grimme S. 2012. Dispersion-corrected density functional theory for aromatic interactions in complex systems. *Accounts Chem. Res.* 46: 4, 916-926. <https://www.pubs.acs.org/accounts> 10.1021/ar3000844

- [8] Kania S. 2014. Hole drift mobility of anthrone and anthrachinone layers with different structures. *Sci. Bull. Techn. Univ. Lodz, Physics*, 35: 17-24. <http://cybra.lodz.pl/dlibra/publication/15667/edition/12516/content>
- [9] Kania S., Kuliński J., Sikorski D. 2018. The origin of the interaction responsible for the difference of hole mobility of two derivatives of anthracene. *Sci. Bull. Techn. Univ. Lodz, Physics*, 39: 27-35. <https://doi.org/10.34658/physics.2018.39.27-35>
- [10] Gaussian 09, Revision A.02. 2009. Frisch M.J., Trucks G.W., Schlegel H.B., Scuseria G.E., Robb M.A., Cheeseman J.R., Scalmani G., Barone V., Mennucci B., Petersson G.A., Nakatsuji H., Caricato M., Li X., Hratchian H.P., Izmaylov A.F., Bloino J., Zheng G., Sonnenberg J.L., Hada M., Ehara M., Toyota K., Fukuda R., Hasegawa J., Ishida M., Nakajima T., Honda Y., Kitao O., Nakai H., Vreven T., Montgomery J.A., Peralta Jr., J.E., Ogliaro F., Bearpark M., Heyd J.J., Brothers E., Kudin K.N., Staroverov V.N., Kobayashi R., Normand J., Raghavachari K., Rendell A., Burant J.C., Iyengar S.S., Tomasi J., Cossi M., Rega N., Millam J.M., Klene M., Knox J.E., Cross J.B., Bakken V., Adamo C., Jaramillo J., Gomperts R., Stratmann R.E., Yazyev O., Austin A.J., Cammi R., Pomelli C., Ochterski J.W., Martin R.L., Morokuma K., Zakrzewski V.G., Voth G.A., Salvador P., Dannenberg J.J., Dapprich S., Daniels A.D., Farkas O., Foresman J.B., Ortiz J.V., Cioslowski J., Fox D.J., Wallingford CT: Gaussian, Inc.
- [11] Skobel'tsyn D.V. 1966. Chapter III The oriented gas model and its application to molecular crystals polarization diagrams of luminescence. in: *Physical optics. The Lebedev Physics Institute series*. 25: 44-66. https://doi.org/10.1007/978-1-4684-7206-6_3
- [12] Choi S.-I., Jortner J., Rice S.A., Silbey R. 1964. Charge transfer exciton states in aromatic molecular crystals. *J. chem. phys.* 41: 3294-3306. <http://dx.doi.org/10.1063/1.1725728>
- [13] Fu Y. 1998. Temperature dependence of the rigid-body motion of anthraquinone. *Acta Cryst. B54*, 308-315. <https://doi.org/10.1107/S0108768197013414>
- [14] Srivastava S.N. 1962. Crystal structure of anthrone. *Z. Krist.* 117: 5-6, 386-398. <https://doi.org/10.1524/zkri.1962.117.5-6.386>

POLARYZACJA CZĄSTECZKI AROMATYCZNEJ W STANIE ANIONU I KATIONU

Streszczenie

Wyniki obliczeń jednoznacznie wskazują na dużą stabilność kationów antrachinonu i antronu. Realizacja przewodnictwa dziur jest w tej sytuacji możliwa dla obu materiałów. Wysoka dodatnia wartość poziomów LUMO

i LUMO+1 dla antrachinonu powyżej 1,8 eV nie pozwala na uzyskanie stabilnego przewodzenia elektronów w fazie stałej antrachinonu. Jednak ujemna wartość poziomu HOMO dla anionu pozwala na przejście cząsteczki w fazie stałej do podstawowego poziomu anionu w stanie jonizacji +1. Pozwala to na wykorzystanie antrachinonu w postaci fazy stałej dla potrzeb technologii wykorzystującej środowisko elektrochemiczne. Wysoka wartość dodatnia poziomów HOMO oraz LUMO i LUMO +1 dla anionu antronu utrudnia uzyskanie efektywnego przewodzenia elektronów dla zastosowań w technologii elektroniki organicznej. Jednak dzięki posiadaniu podstawnika, własności anionu antronu są korzystniejsze dla zastosowań niż własności anionu niepodstawionego antracenu. Pomimo podobieństwa cząsteczek i struktur, w jakich krystalizują, występuje znacząca różnica w wartości przerwy energetycznej E_g pomiędzy antronem i antrachinonem. Uzyskane wyniki wskazują na inne obszary możliwych zastosowań antrachinonu i antronu w elektronice organicznej. Wysoka wartość energii przerwy zabronionej może być korzystna dla zastosowań obu materiałów do wytwarzania warstw aktywnych w komórkach słonecznych, gdzie wymagana jest wysoka rezystywność ze względu na konieczność rozdziału generowanych ładunków.

**SYLWESTER KANIA^{1,2}, BARBARA KOŚCIELNIAK-MUCHA²
JANUSZ KULIŃSKI², PIOTR SŁOMA²
KRZYSZTOF WOJCIECHOWSKI²**

¹ Institute of Physics, Lodz University of Technology, ul. Wólczańska 219,
90-924 Łódź, Poland, e-mail: sylwester.kania@p.lodz.pl

² Centre of Mathematics and Physics, Lodz University of Technology,
al. Politechniki 11, 90-924 Łódź, Poland, e-mail: janusz.kulinski@p.lodz.pl

CHARGE CARRIER MOBILITY IN NON-EQUILIBRATED TRANSPORT IN MOLECULAR MATERIALS

Non-equilibrated transport of charge carriers in the molecular material depends on the structure and packing of the molecules. Explanation of the measurements of the photocurrent generated with use of UV flash light in organic layer needs to define the quantity of charge carriers mobility. Definition of this quantity in the scope of some defined transport model requires the detailed analysis of generation, recombination and charge transfer between neighbouring molecules. The problem is discussed on the basis of transport properties of two anthracene derivatives.

Keywords: charge transfer mobility, photocurrent, hopping transport, Marcus-Hush theory.

1. INTRODUCTION

Nowadays, molecular electronics requires new research aimed at development of the technology of new low-weight organic semiconducting materials. This technology allows the optimal usage of their strengths, *i.e.* low production costs, flexibility, low molecular weight, the ability to modulate their properties by changing the structure of the molecule leading to proper space charge distribution in molecule favourable for strengthening π - π interactions. Organic semiconductors can be used to produce the continuous and homogeneous layers with a large surface in terms of large scale production

technology [1]. The essential stage for research in the field of organic electronics is determining the potential of organic semiconductor material properties for their adaptation in practice [2, 3].

The mobility of charge carriers is an important parameter used to determine the potential applications of the organic semiconductor. Experimental measurement of this quantity requires the construction of a measuring cell in which metallic contacts attached to the layer of the measured organic material play an important role. Although the mobility of the charge carriers is a quantity characterizing a given material, the obtained result of mobility is always dependent on the method of performing this measurement [4,5]. Therefore, appropriate theoretical methods of description are sought. They will allow estimation of the value of charge carrier mobility, as a material constant.

Preliminary X-ray examinations can be helpful to determine the properties of the transport of charge carriers in organic material. Conventional X-ray structural analysis tries to develop the description of the ideal internal structure of crystalline bodies. The limitation of this method is the fact that it is based on the assumption that the electron density of the atom in the crystal is well described by spherical averaging of the electron density of individual atoms [6]. Diffraction methods belong to the group of indirect methods that allow obtaining structural data after appropriate mathematical processing of the recorded measurement data. This means that the diffraction pattern is obtained by averaging the electron density distribution of many atoms (at least on the order of 10^{18} atoms per diffractogram). As a result, the crystal is considered to be composed of isolated non-interacting atoms. Of course, additional X-ray analysis allows inferences about existing bonds. An additional limitation of the X-ray method is that reduction of measurement temperature is required to reduce the thermal movement of atoms for accurate analysis of diffraction data. In practice, however, organic electronics devices most often work in the range from room temperatures to about 80 °C. Therefore, it is helpful to calculate electrical properties in a theoretical way in order to determine the electrical properties of the organic material at the molecular level. Theoretical calculations using quantum-chemical calculations allow for an accurate description of the molecular orbitals of a single molecule or molecules in a unit cell at any temperature. Such calculations using GAUSSIAN 09 package software [7] were carried out by our team previously in the case of unit cells made of anthrone and anthraquinone particles [8,9]. These two anthracene derivatives can be used in the form of layers to produce organic field effect transistors (OFET) [10]. Anthrone and anthraquinone are two derivatives of anthracene similar in shape. They can be considered as a model set of two compounds crystallizing in almost identical structures and with almost identical molecules but differing in presence

of permanent dipole moment. The anthrone molecule possesses a significant natural dipole moment, and when measured in benzene is of 3.66 D ($1.22 \cdot 10^{-29}$ Cm), but anthraquinone possesses much lower value of natural dipole moment when measured in benzene of 0.6 D ($2.00 \cdot 10^{-30}$ Cm) [11]. Our previous researches were related to the evaluation of the molecule geometry change during charge carrier transport. The main result of calculations revealed that the difference between the hole mobility for both materials was due to the presence of permanent dipole moment. Permanent dipole moment in the gas phase is present only in the case of anthrone molecule. In this paper we want to check whether the direct application of the Marcus-Hush model with the two anthracene derivative compounds would allow for explanation of differences in measured mobility values.

1.1. Mobility in diabatic and adiabatic processes

The mobility of charge carriers is defined as the charge carrier velocity induced by external unit value of electric field. In solid, it is a tensor quantity, μ_{ij} , describing the relationship between vector components of averaged charge carrier velocity $\langle v \rangle_i$ and components E_j of the vector of external electric field

$$\mu_{ij} = \langle v \rangle_i / E_j . \quad (1)$$

For amorphous materials it may be assumed that macroscopic mobility is considered as a scalar quantity

$$\mu = \langle v \rangle / E \quad (2)$$

This assumption takes into account the disorder of the positions of the molecules relative to each other and energy disorder. The thermal vibrations that interfere with the transfer of charges between adjacent molecules are the source of disorder, even in crystalline materials at temperatures close to applications of organic electronics, *i.e.* at room temperatures (RT). This results in the localization of charge carriers. Such an effect destroys the translational symmetry of the system making the description of band conduction inadequate for the charge carrier transport phenomena at RT [12]. Calculation shows that the fluctuations in the amplitudes of the transfer integrals are of the same order as their average values [13].

Mobility can be determined experimentally by time of flight (TOF) measurements. Measurement using the apparatus applied in this method allows for direct measurement of time of flight in the case of weak dispersion [14]. Therefore, no relationship between the transit time of the charge carriers through the layer and the applied external electric field is observed in the case of strong

dispersion. In the latter case, the observed transit time of the carriers is interpreted as a life-time of the carriers [15, 16]. Therefore, either the drift mobility value or the mobility value determined by the Einstein equation after determining the diffusion constant value can be obtained as a result of such measurement.

The drift mobility in TOF experiment with the weak dispersion is defined as

$$\mu_{TOF} = L / (Et_{tr}). \quad (3)$$

Here, t_{tr} is the time of flight, determined experimentally from observed shape of transit currents for the organic layer with thickness L .

In turn, the value of the observed lifetime allows determination of the diffusion constant D of charge carriers [15,16]. Value of this constant allows to calculate the Einstein mobility based on Einstein's dependence

$$\mu = (e/k_B T) D, \quad (4)$$

where e is a charge of the charge carrier, k_B is the Boltzmann constant and T is the absolute temperature. Calculation of the mobility of charge carriers in high-resistance organic material is difficult because the influence of an external electric field and the thermal interaction of molecules modify electronic states. Even for a qualitative description, a number of simplifications are required. Conduction in organic material occurs through a spatially extended molecule and then as a result of diffusion of the charge carrier between adjacent molecules. In the case of organic material, the theoretical description of charge carrier transport is facilitated because the weak intermolecular interactions (of the order of 0.4-0.8 eV/molecule) which allows to consider the interactions important for conductivity as interactions between pairs of neighbouring molecules. This fact allows to omit the crystal structure of the tested material in theoretical calculations [17].

Theoretical estimation of mobility in the absence of an electric field is possible on the basis of Marcus-Hush theory [17]. This theory allows the calculation of parameters associated with the change of spatial distribution of the electron density of a molecule when transfer of charge carrier occurs. The energy factor associated with the deformation of a molecule during charge transfer is called reorganization energy and the factor associated with the transfer of charge carriers is the transfer integral. Marcus-Hush theory uses a diabatic description of charge transfer. The diabatic description assumes that changes in the state extracted from the environment of the thermodynamic system may occur in the path of the exchange of energy with the environment under the conditions of infinitesimally small energy difference between them.

In turn, the competitive adiabatic process progresses as a result of thermodynamic changes which are associated with relaxation of the disturbed system to a state of equilibrium without heat exchange with the environment. The rate of hole transfer between two adjacent molecules, k_e , during the charge carrier transport can be defined on the basis of Marcus – Hush theory [12,18] as:

$$k_e = \left(4\pi^2/h\right) \left(J^2 \exp(-E_r/(4k_B T))\right) / \sqrt{4\pi \cdot E_r k_B T}, \quad (5)$$

where h is Planck constant, E_r is the reorganization energy and J is the charge transfer integral.

2. CALCULATIONS AND DISCUSSION

The quantum-chemical calculations were carried out with use of density functional theory (DFT) with GAUSSIAN09 program [7]. The structures of anthraquinone and anthrone were optimized at B3LYP (Becke three parameter (exchange), Lee Yang, and Parr) method using 6-311+g(d,p) basis set. Based on the optimized geometric structure, the energy of high occupied molecular orbital (HOMO), and energy of low unoccupied molecular orbital (LUMO) and band gap calculations were performed with the same level of theory at the ground state and cation and anion state for the molecules being in the gas. We calculated reorganization energy E_r and charge transfer integral J in the manner similar to shown in [19]. The results of calculations are presented in the Table 1. For comparison, apart from anthrone and anthraquinone, the calculation results for anthracene are shown.

Table 1
Calculated reorganization energy E_r , charge transfer integral J and rate of charge transfer k_e for anthrone, anthraquinone and for anthracene

		Anthrone	Anthraquinone	Anthracene
E_r , holes	[eV]	0.174	0.135	0.139
E_r , electrons	[eV]	0.371	0.354	0.198
J , holes	[eV]	0.111	0.092	0.611
J , electrons	[eV]	0.600	0.564	0.337
k_e , holes	[Hz]	$9.29 \cdot 10^{13}$	$1.02 \cdot 10^{14}$	$4.35 \cdot 10^{15}$
k_e , electrons	[Hz]	$2.73 \cdot 10^{14}$	$2.92 \cdot 10^{14}$	$6.28 \cdot 10^{14}$

To describe the diffusion process, it is necessary to estimate the diffusion constant D of charge carriers [17,19]. If the charge carrier transfer rate between two molecules obtained on the basis of the Marcus-Hush formula is k_e , then the

estimation of the diffusion constant for the conductivity of holes requires the use of the expression similar as in [20,21] when taking into account the amorphous structure of the layer:

$$D = (1/(2nM))(L^2 k_e / L_k), \quad (6)$$

where n is the dimensionality of the transport process (we assume here that $n = 3$), L_k is the number of possible charge carrier transfers to neighbouring molecules, M is a number of independent molecules in the unit cell, k_e is the rate of charge transfer equation (5), L is the effective distance between centroids (center of mass) of neighbouring molecules.

Using equation (6), assuming that the parameter $L \cong 4 \text{ \AA}$ [17], and using the calculated values of carrier transfer rate k_e for anthrone and anthraquinone, $9.29 \cdot 10^{13} \text{ Hz}$ and $1.02 \cdot 10^{14} \text{ Hz}$, respectively, we obtain, based on formula (4), the mobility of the holes which is about $1.7 \cdot 10^{-2} \text{ cm}^2/\text{Vs}$ for both materials. Mobility of the electrons for both materials calculated in the same manner is equal to $4.7 \cdot 10^{-2} \text{ cm}^2/\text{Vs}$.

Table 2

Experimental hole [14] and electron [22] mobility for anthrone and anthraquinone for amorphous layers and calculated for the values from Table 1 with use Eqs. (4) and (6)

Compound	Type of charge carrier	Structure	Experimental μ [cm^2/Vs]	Calculated, μ [cm^2/Vs]
anthraquinone	hole	amorphous	$(0.9-6.0) \cdot 10^{-4}$	$1.7 \cdot 10^{-2}$
anthrone	hole	amorphous	$(0.6-4.0) \cdot 10^{-3}$	$1.7 \cdot 10^{-2}$
anthraquinone	electron	amorphous		$4.7 \cdot 10^{-2}$
anthrone	electron	amorphous	$(0.6-3.0) \cdot 10^{-3}$	$4.7 \cdot 10^{-2}$

Table 2 compares the experimental mobility values for the amorphous layers of anthrone and anthraquinone with the mobility values calculated using data from Table 1 with use of formulas (4) and (6). Both the experimental and calculated mobility values for both compounds are at least two orders of magnitude smaller than the value of $1 \text{ cm}^2/\text{Vs}$, which is the limit value above which the transport of charge carriers is a band transport. Therefore, the calculated mobility values allow us to assume that for both compounds we are dealing with hopping transport. This assumption is valid for both holes and electrons.

3. CONCLUSIONS

Mobility values calculated using Marcus-Hush theory for both materials with similar molecules and almost identical crystal packing are almost identical. However, the empirical mobilities for both compounds are different almost by an order of magnitude. We think that the reason for this difference in the mobilities determined experimentally for both compounds is the presence of a permanent dipole moment in the anthrone molecule and its absence in the anthraquinone molecule. To ensure better correlation of the calculations with the experimental results, it is necessary to consider factors that may influence on the value of the estimated diffusion constant of charge carriers and may influence on the value of the calculated transfer integral. More accurate calculations must take into account the presence of a constant dipole moment in the anthrone molecule because the presence of this moment creates an additional interaction between the anthrone molecules comparable with the energy of van der Waals interactions.

Despite the simplicity of theoretical considerations applied in this paper, the obtained calculation results give a qualitatively correct picture of transport. For both materials, *i.e.* anthrone and anthraquinone, the mobility values obtained from Marcus-Hush theory for both hole transport and electron transport are in the range of hopping transport.

4. ACKNOWLEDGEMENTS

The calculations mentioned in this paper are performed using the PLATON project's infrastructure at Lodz University of Technology Computer Centre.

REFERENCES

- [1] Kwon J., Takeda Y., Shiwaku R., Tokito S., Cho K., Jung S. 2019. Three-dimensional monolithic integration in flexible printed organic transistors. *Nat. commun.*, 10: 54-1-54-9. <https://doi.org/10.1038/s41467-018-07904-5>
- [2] Irfan A., Al-Sehemi A., A Assiri M., Mumtaz M.W. 2019. Exploring the electronic, optical and charge transfer properties of acene-based organic semiconductor materials. *Bull. matter. sci.* 42: 145-1–145-7.
- [3] Wazzan N., Irfan A. 2018. Theoretical study of triphenylamine-based organic dyes with mono-, di-, and tri-anchoring groups for dye-sensitized solar cells. *Org. electr.* 63: 328-342. <https://doi.org/10.1016/j.orgel.2018.09.039>

- [4] Blakesley J.C., Castro F. A., Kylberg W., Dibb G. F.A., Arantes C., Valaski R., Cremona M., Kim J. S., Kim J.-S. 2014. Towards reliable charge-mobility benchmark measurements for organic semiconductors. *Org. electr.* 15: 1263-1272. <http://dx.doi.org/10.1016/j.orgel.2014.02.008>
- [5] de Boer R.W.I., Jochemsen M., Klapwijk T.M., Morpurgo A.F. 2004. Space charge limited transport and time of flight measurements in tetracene single crystals: a comparative study. *J. appl. phys.* 95: 3, 1196-1202. <https://doi.org/10.1063/1.1631079>
- [6] Slouf M. 2002. Determination of net atomic charges in anthraquinone by means of 5-h X-ray diffraction experiment. *J. mol. struct.* 611: 1-3, 139-146. [https://doi.org/10.1016/S0022-2860\(02\)00060-1](https://doi.org/10.1016/S0022-2860(02)00060-1)
- [7] Gaussian 09, Revision A.02. 2009. Frisch M.J., Trucks G.W., Schlegel H.B., Scuseria G.E., Robb M.A., Cheeseman J.R., Scalmani G., Barone V., Mennucci B., Petersson G.A., Nakatsuji H., Caricato M., Li X., Hratchian H.P., Izmaylov A.F., Bloino J., Zheng G., Sonnenberg J.L., Hada M., Ehara M., Toyota K., Fukuda R., Hasegawa J., Ishida M., Nakajima T., Honda Y., Kitao O., Nakai H., Vreven T., Montgomery J.A., Peralta Jr. J.E., Ogliaro F., Bearpark M., Heyd J.J., Brothers E., Kudin K.N., Staroverov V.N., Kobayashi R., Normand J., Raghavachari K., Rendell A., Burant J.C., Iyengar S.S., Tomasi J., Cossi M., Rega N., Millam J.M., Klene M., Knox J.E., Cross J.B., Bakken V., Adamo C., Jaramillo J., Gomperts R., Stratmann R.E., Yazyev O., Austin A.J., Cammi R., Pomelli C., Ochterski J.W., Martin R.L., Morokuma K., Zakrzewski V.G., Voth G.A., Salvador P., Dannenberg J.J., Dapprich S., Daniels A.D., Farkas O., Foresman J.B., Ortiz J.V., Cioslowski J., Fox D.J., Wallingford CT: Gaussian, Inc.
- [8] Kania S., Kościelniak-Mucha B., Kuliński J., Słoma P. 2016. The effect of symmetry of a molecule electronic density on the dipole moment of unit cell and hole conductivity of thin polycrystalline films of anthrone and anthraquinone. *Sci. bull. techn. univ. lodz, physics*, 37: 49-64. <https://doi.org/10.34658/physics.2016.37.49-64>
- [9] Kania S., Kościelniak-Mucha B., Kuliński J., Słoma P. 2015. Effect of molecule dipole moment on hole conductivity of polycrystalline anthrone and anthrachinone layers. *Sci. bull. techn. univ. lodz, physics*, 36: 13-26. <http://cybra.lodz.pl/dlibra/publication/17133/edition/13805/content>
- [10] Yan L., Qi M., Li A., Meng H., Zhao X., Ali M., Xu B. 2019. Investigating the single crystal OFET and photo-responsive characteristics based on an anthracene linked benzo[b]benzo[4,5]thieno[2,3-d]thiophene semiconductor. *Org. electr.* 72: 1-5. <https://doi.org/10.1016/j.orgel.2019.05.039>
- [11] Landolt-Börnstein. 1971. *Zahlenwerte und Funktionen aus Naturwissenschaften und Technik*, Berlin:Springer Verlag.
- [12] Troisi A., Orlandi G. 2006. Charge- transport regime of crystalline organic semiconductors: diffusion limited by thermal off-diagonal electronic disorder. *Phys. rev. lett.* 96: 086601-1-086601-4. DOI: 10.1103/PhysRevLett.96.086601
- [13] Troisi A., Orlandi G., Anthony J.E. 2005. Electronic interactions and thermal disorder in molecular crystals containing cofacial pentacene units. *Chem. mater.* 17: 5024-5031. <https://pubs.acs.org/doi/pdf/10.1021/cm051150h>

- [14] Kania S. 2014. Hole drift mobility of anthrone and anthrachinone layers with different structures. *Sci. bull. techn. univ. lodz, physics*, 35: 17-24. <http://cybra.lodz.pl/dlibra/publication/15667/edition/12516/content>
- [15] Kania S., Dłużniewski M. 2005. Charge carrier lifetime in DLC films, *Diamond & related materials* 14: 1, 74-77. <https://doi.org/10.1016/j.diamond.2004.07.015>
- [16] Fritzsche H., *Proc. Int. Summer School on Semiconductors, ESPOO, Helsinki*, 1982, p. 2.
- [17] Datta A., Mohakud S., Pati S.K. 2007. Electron and hole mobilities in polymorphs of benzene and naphthalene: role of intermolecular interactions. *J. Chem. Phys.* 126: 144710-1-144710-6. <https://doi.org/10.1063/1.2721530>
- [18] Kania S., Kuliński J., Sikorski D. 2018. The origin of the interactions responsible for the difference of hole mobility of two derivatives of anthracene. *Sci. bull. techn. univ. lodz, physics*, 39: 27-35. <https://doi.org/10.34658/physics.2018.39.27-35>
- [19] Deng W-Q., Goddard III W.A. 2004, Predictions of hole mobilities in oligoacene organic semiconductors from quantum mechanical calculations. *J. phys. chem. B* 108: 8614-8621. <https://pubs.acs.org/toc/jpcb/108/25>
- [20] Wen S.-H., Li A., Song J., Deng W.-Q., Han K.-L., Goddard III W.A. 2009. First-principles investigation of anisotropic hole mobilities in organic semiconductors. *J. phys. chem. B* 113: 8813-8819. <https://pubs.acs.org/doi/10.1021/jp900512s>
- [21] Köhler A., Bässler H. 2011. What controls triplet exciton transfer in organic semiconductors? *J. mater. chem.* 21: 4003-4011. <https://doi.org/10.1039/c0jm02886j>
- [22] Kania S. 2009. Electron drift mobility in amorphous anthrone layers. *Sci. Bull. Techn. Univ. Lodz, Physics*, 30: 65-72. <http://cybra.lodz.pl/dlibra/doccontent?id=3532>

RUCHLIWOŚĆ NOŚNIKÓW ŁADUNKU W PRZEWODNICTWIE NIERÓWNOWAGOWYM MATERIAŁÓW MOLEKULARNYCH

Streszczenie

Opis nierównowagowego transportu nośników ładunku w warunkach fotoprądu wzbudzanego impulsem światła wymaga zdefiniowania ruchliwości nośników ładunku. Definicja tej wielkości w odniesieniu do określonego modelu transportu wymaga wnikliwej analizy procesów generacji, rekombinacji i transferu ładunku pomiędzy sąsiadującymi cząsteczkami. W tej pracy do opisu transportu nośników ładunku w antronie i antrachinonie wykorzystano teorię Marcusa–Husha, która dotyczy transportu hoppingowego. Uzyskano prawie identyczne wartości ruchliwości dziur w obu materiałach, tj. $1,7 \cdot 10^{-2} \text{ cm}^2/\text{Vs}$ oraz identyczne wartości ruchliwości elektronów $4,7 \cdot 10^{-2} \text{ cm}^2/\text{Vs}$. Pomimo prostoty rozważań teoretycznych uzyskane wyniki

obliczeń dają jakościowo poprawny obraz transportu, zgodny z wynikami doświadczalnymi. Dla obu związków wartości ruchliwości obliczone za pomocą teorii Marcusa-Husha zarówno dla transportu dziur jak i dla transportu elektronów są w zakresie transportu hoppingowego.

ISSN 1505-1013

e-ISSN 2449-982X

<http://cybra.lodz.pl/publication/3923>

<http://eczasopisma.p.lodz.pl.PHYSICS/issue/archive>